Extremal size fluctuations in QCD dipole cascading

R. Enberg* and R. Peschanski†
Service de Physique Théorique, CEA/Saclay, 91191 Gif-sur-Yvette Cedex, France‡

The statistics of *extremal* (minimal and maximal) dipole sizes in the QCD wave function of an onium system is shown to be governed by a non-linear equation in rapidity. It has the same form as the Balitskiĭ-Kovchegov (BK) equation with different initial conditions for the minimal and maximal cases. The minimal dipole size is shown to shrink towards the ultraviolet at the same rate as the BK saturation radius. The maximal dipole size scales differently and rapidly towards the infrared demonstrating significantly large dipole size fluctuations, strikingly sensitive to next-to-leading corrections. Numerical simulations performed of the Fourier modes confirm the analytic predictions based on traveling wave asymptotic solutions. The large fluctuations revealed by extremal size statistics may have important consequences for QCD saturation.

I. INTRODUCTION

The perturbative QCD linear evolution equation in rapidity Y for two-body amplitudes is referred to as the Balitskiĭ–Fadin–Kuraev–Lipatov (BFKL) equation [1]. It can be derived using the QCD wave function of an onium (a massive $q\bar{q}$ state). This wave function specifies a distribution of color singlet dipoles [2, 3] in the onium state, and the evolution can be described [2] by the cascading of $q\bar{q}$ color singlet dipoles, splitting and evolving in a branching process such as the one sketched in Fig. 1. The BFKL amplitudes are obtained by computing the scattering of dipoles present in this wave function at a given rapidity. In transverse space, the splitting probability per unit of rapidity is defined by the BFKL kernel

$$\mathcal{K}(x_0, x_1; x_2) = \frac{\alpha_s N_c}{\pi} \frac{x_{01}^2}{x_{02}^2 x_{12}^2} \ , \tag{1}$$

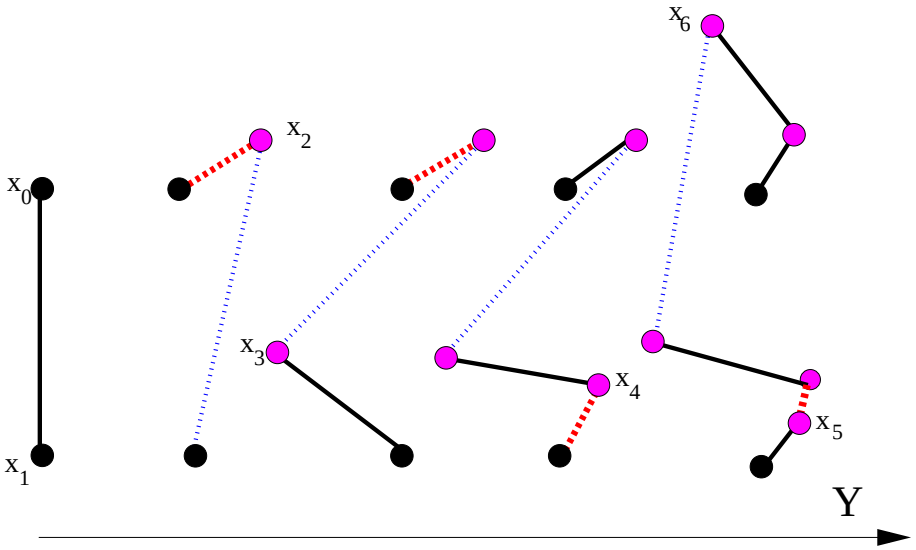

FIG. 1: *Dipole branching process.* The figure shows the rapidity evolution of one dipole (x_0, x_1) after successive splitting at $x_2, x_3, ..., x_6$. At each step the *minimal* size is indicated by a dashed line, the *maximal* size by a dotted line. Note that the largest and smallest dipoles in each step are not necessarily daughters of the largest or smallest dipoles in the preceding step.

‡ URA 2306, Unité de recherche associée au CNRS.
*Electronic address: REnberg@lbl.gov;
Present address: Theoretical Physics Group, Lawrence Berkeley National Laboratory, Berkeley, CA 94709, USA
†Electronic address: pesch@spht.saclay.cea.fr

where α_s is the QCD coupling constant, x_i are the endpoint coordinates of the dipoles in two-dimensional transverse space, and $x_{ij} = x_i - x_j$. Hence an initial dipole (x_0, x_1) splits into two dipoles, the process repeating itself as a function of rapidity, see Fig. 1. Note that the regularization of the kernel singularities at the end-points is provided by a virtual contribution expressing the probability of no branching [2].

The onium wave function appears as a major tool in various interesting physical questions concerning high-energy QCD. It is an ingredient in the calculation of the onium–onium scattering amplitude in the dipole framework [2], where it has been shown to be proportional to the dipole size density. It is also present in saturation problems [4], where the BFKL kernel (1) appears again, but now in the non-linear framework of the Balitskiĭ–Kovchegov (BK) equation [5, 6] where it incorporates the damping of the onium scattering S-matrix element $0 \leq \mathcal{S}(x_{01}, Y) \leq 1$ on a large nucleus due to unitarity. The original BFKL evolution equation is obtained by writing $\mathcal{S} = 1 - \mathcal{T}$ and keeping only linear terms in $\mathcal{T}$. Recently, analytic asymptotic solutions of the non-linear equation have been found in terms of traveling waves [7], corresponding to the "geometric scaling" property $\mathcal{S}(x_{01}, Y) \sim \mathcal{S}\left(x_{01} Q_s(Y)\right)$ proposed earlier on phenomenological grounds [8].

The expression for the total onium scattering amplitudes in the BFKL (linear) regime can be derived from the dipole size distribution in the onium wave function [2]. The solutions of the BK equation are also dependent on the linear regime [7] since the non-linearities appear essentially as a selection mechanism among linear solutions. However, other interesting features of high energy QCD observables seem to depend on the fluctuation patterns of the dipole cascade. This is not described by the BK equation, which is a kind of mean field approximation. Some typical examples where fluctuations are important are, e.g., the multiplicity distribution of dipoles [9] and the solution of the evolution equation in the deep saturation region $\mathcal{S} \to 0$ where the BK solution [10] is being modified by rare fluctuations [11]. More generally the quest for solutions of the QCD saturation equations beyond the BK approximation [5, 12] seem to point to the consideration of modifications taking into account fluctuations of the dipole cascade, see e.g. [13].

The aim of this work is to take a step towards the theoretical study of fluctuations in QCD dipole cascading. It will allow exhibiting new aspects of the QCD dipole cascade which have not been yet studied analytically, while implicitly present in numerical simulations [9]. For this sake, we will take advantage of the identification of QCD dipole cascading with a stochastic branching process governed by the kernel (1). As such, it obeys some remarkable mathematical properties which we will address and adapt to the physical case of QCD cascading. We focus on the properties of *extreme value statistics* in branching processes which have been the subject of many studies in statistical physics [14]. Extreme value statistics characterize the maximal and minimal values taken by random variables. In the case of random variables associated to branching processes, such as the lengths obtained by successive random splitting of a segment, this problem is already non trivial [14] due to the strong correlations induced by the branching.

In our case, we will focus on the statistics of the maximum and minimum dipole sizes, $r_M \equiv \max |x_{k,k+1}|$ and $r_m \equiv \min |x_{k,k+1}|$, where x_k are the splitting points at given rapidity Y. We will study these statistics as a function of Y, which is taken here as the evolution variable. These distributions encode the maximal extent of size fluctuations encountered during the QCD dipole cascading with energy. A schematic example is given in Fig.1, exhibiting sizable fluctuations of the dipole sizes already in one cascading event.

While the QCD cascade is conceptually similar to the cases considered in statistical physics, new aspects have to be treated, such as the two-dimensional features of coordinate space and the singularities of the kernel whose origin is deeply rooted in QCD properties. This leads to different types of equation and solutions, which we shall investigate.

The plan of our paper is the following. In section II we define the general framework of extreme value statistics and derive the evolution equation obeyed by the extreme dipole size distributions. In section III, we formulate the problem in terms of the Fourier modes of the size distribution, useful for numerical analysis. In section IV, we first focus on the *minimal* size problem and derive the solutions of the corresponding equations, and in section V the new and more involved treatment of the *maximal* size distribution is presented. In section VI we solve the same equations numerically and study the solutions. Conclusions and outlook are given in section VII.

II. EXTREME VALUE STATISTICS

Let us define the probability distributions for the *minimal* and *maximal* size of dipoles emanating from an initial dipole of location x_{01} at Y_0, namely

$$\begin{aligned} \text{Min:} \qquad \mathcal{P}(x_{01}, r, Y) &\equiv \text{Prob}\left\{x_{01} \to r_k > r, \forall k \text{ at rapidity } Y\right\} \\ \text{Max:} \qquad \mathcal{Q}(x_{01}, r, Y) &\equiv \text{Prob}\left\{x_{01} \to r_k < r, \forall k \text{ at rapidity } Y\right\} \end{aligned} \tag{2}$$

and their complements

$$\begin{aligned} \mathcal{N}(x_{01}, r, Y) = 1 - \mathcal{P} &\equiv \text{Prob}\left\{\exists k, x_{01} \to r_k \leq r \text{ at rapidity } Y\right\} \\ \mathcal{M}(x_{01}, r, Y) = 1 - \mathcal{Q} &\equiv \text{Prob}\left\{\exists k, x_{01} \to r_k \geq r \text{ at rapidity } Y\right\} \ . \end{aligned} \tag{3}$$

These probability distributions verify a straightforward algebra, in particular, one has $\mathcal{P}\times\mathcal{Q}\sim 0$, hence $\mathcal{N}\times\mathcal{M}=(1-\mathcal{P})\times(1-\mathcal{Q})\sim 1-\mathcal{P}-\mathcal{Q}$ has the physical meaning of the probability for having fluctuating dipole sizes both below and above the value r at rapidity Y.

The boundary conditions are defined by the size distribution of the initial dipole configurations in the onium. To give a simple explicit example, let us consider the case of a distribution well peaked around a dipole x_{01}. Then the boundary conditions can be approximated by step functions, namely

$$\mathcal{P}(x_{01},r,Y_0)=\theta(L)\qquad \mathcal{Q}(x_{01},r,Y_0)=\theta(-L) \tag{4}$$

$$\mathcal{N}(x_{01},r,Y_0)=\theta(-L)\qquad \mathcal{M}(x_{01},r,Y_0)=\theta(L), \tag{5}$$

where $L\equiv\log\left(r_0^2/r^2\right)$. By a dimensional argument, $\mathcal{P},\mathcal{Q}$ (and $\mathcal{N},\mathcal{M}$) depend only on the ratio r_0/r when the impact parameter dependence is neglected[1]. More generally we will consider smeared distributions around θ functions. In physical terms, the distributions $\mathcal{P}$ and $\mathcal{N}$ characterize the propagation of extreme dipole sizes towards small sizes, i.e. the "ultraviolet", starting from an initial distribution centered around x_{01}. On the other hand, the distributions $\mathcal{Q}$ and $\mathcal{M}$ determine the evolution of extreme large dipole sizes. We will see that in fact there is an evolution in the other direction towards larger sizes, i.e. the "infrared".

The evolution equations for both probability distributions $\mathcal{P}$ and $\mathcal{Q}$ are obtained from the observation that during the rapidity interval $Y\to Y+dY$ the probability for satisfying the extremal conditions (2) comes from a twofold constraint: It must not change in the absence of branching, while it must still be satisfied by the two split dipoles x_{02} and x_{12} in the case of a branching happening in the rapidity interval dY and space volume d^2x_2. Thus, e.g. for $\mathcal{P}$, we consider the two possibilities that either the dipole remains intact, with probability $1-\mathcal{K}(x_0,x_1;x_2)\,dY\,d^2x_2$, or it splits with probability $\mathcal{K}(x_0,x_1;x_2)\,dY\,d^2x_2$. This yields the probability relation

$$\mathcal{P}(x_{01},r,Y+dY)=\left[\mathcal{K}(x_0,x_1;x_2)\,dY\,d^2x_2\right]\mathcal{P}(x_{02},r,Y)\mathcal{P}(x_{12},r,Y)+\left[1-\mathcal{K}(x_0,x_1;x_2)\,dY\,d^2x_2\right]\mathcal{P}(x_{01},r,Y), \tag{6}$$

which, taking the limit $dY\to 0$ and integrating over d^2x_2, yields

$$\frac{\partial\mathcal{P}}{\partial Y}(x_{01},r,Y)=\int d^2x_2\;\mathcal{K}(x_0,x_1;x_2)\;\left\{\mathcal{P}(x_{02},r,Y)\mathcal{P}(x_{12},r,Y)-\mathcal{P}(x_{01},r,Y)\right\}. \tag{7}$$

It is clear from this argument that $\mathcal{Q}$ obeys the same equation. To be careful, a small parameter could have been introduced as a cut-off to avoid the divergences in the splitting probability $\int_\rho dx_2\;\mathcal{K}(x_0,x_1;x_2)$. Interestingly enough, this cut-off can be set to zero in (7), since the combination of both terms in the integrand is regular. This means that the probability distributions $\mathcal{P}$ and $\mathcal{Q}$ are well-defined despite the divergent kernel (1). However, these divergences in the integration measure reflect a deep specific structure of QCD in the dipole formulation. This is at variance with the cases appearing in statistical physics [14], where the kernels are in general finite and one-dimensional.

Performing the replacements $\mathcal{P}\to 1-\mathcal{N}$, $\mathcal{Q}\to 1-\mathcal{M}$, one gets

$$\frac{\partial\mathcal{N}}{\partial Y}(x_{01},r,Y)=\int d^2x_2\;\mathcal{K}(x_0,x_1;x_2)\;\left\{\mathcal{N}(x_{02},r,Y)+\mathcal{N}(x_{12},r,Y)-\mathcal{N}(x_{01},r,Y)-\mathcal{N}(x_{02},r,Y)\times\mathcal{N}(x_{12},r,Y)\right\}\;, \tag{8}$$

and the same for $\mathcal{M}$.

It is remarkable that Eq. (7) is identical to the BK equation for the S-matrix element $\mathcal{S}(x_{01},Y)$. Moreover the "unitarity condition" holds also for $\mathcal{P},\mathcal{Q}$, since they are also probability distributions. Eventually, the only specific characteristics are the initial conditions (4) which we will take into account in the following. We shall discuss later the similarities and differences between the two occurrences of the same mathematical BK equation, the known one being a saturation equation, the one here studied being for the study of fluctuations of the onium wave function in the *linear* BFKL regime.

III. ANALYSIS IN FOURIER MODES

It is well-known [6] that, within the approximation of impact-parameter independence, the BK equation acquires a quite simple form by Fourier transformation over the dipole size $x_{01}\to\boldsymbol{k}$. It is quite useful for the derivation of

[1] However, if one wants to keep track of the transverse space positions, e.g. for a simulation in space, more information on the transverse coordinates of dipoles should be kept, and the equations will have to be modified.

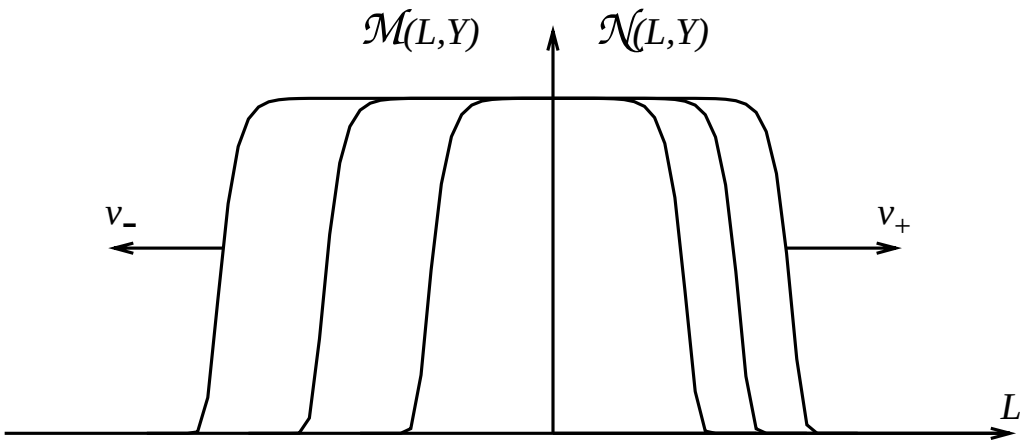

FIG. 2: Traveling wave solutions for the extremal size distributions. The functions $\mathcal{N}, \mathcal{M}$ are represented for three increasing rapidity values. For the *minimal* size distribution $\mathcal{N}$, the wave front connecting the regions $\mathcal{N} = 1$ and $\mathcal{N} = 0$ travels from the left to the right as Y increases. For the *maximal* size distribution $\mathcal{M}$, the traveling wave, when it exists (see section V), travels in the opposite direction, from smaller to larger values of the maximal sizes.

analytical properties [7]. Since we are interested in intrinsic properties of dipole sizes independently of the choice of a reference frame, we are just in the situation of using this framework. Thus we will consider the following transformation

$$\mathcal{T}(k,Y) = \int \frac{d^2x_{01}}{2\pi x_{01}^2} e^{-i<k\cdot x_{01}>} \mathcal{N}(x_{01},Y) = \int_0^\infty \frac{dr}{r} J_0(kr)\ \mathcal{N}(r,Y), \tag{9}$$

where the last equality holds since $\mathcal{N}$ only depends on the magnitude r of x_{01} and thus $\mathcal{T}$ only on k. The equation (8) then takes the form

$$\frac{\partial \mathcal{T}(k,Y)}{\partial Y} = \frac{\alpha_s N_c}{\pi} \left[K \otimes \mathcal{T}(k,Y) - \mathcal{T}^2(k,Y) \right] \tag{10}$$

where the kernel K is the integral kernel of the BFKL equation,

$$K \otimes \mathcal{T}(k,Y) = \int_0^\infty \frac{dk'^2}{k'^2} \left[\frac{k'^2 \mathcal{T}(k',Y) - k^2 \mathcal{T}(k,Y)}{|k^2 - k'^2|} + \frac{k^2 \mathcal{T}(k,Y)}{\sqrt{4k'^4 + k^4}} \right]. \tag{11}$$

The same equation (10) holds for the substitution $\mathcal{T} \to \mathcal{U}$, with $\mathcal{U}$ defined as the Fourier transform of $\mathcal{M}$.

As in the preceding case, the boundary conditions have to be defined according to the propagation of the extrema towards the ultraviolet and the infrared. In terms of Fourier modes k, we will thus define initial conditions which will correspond to initial modes centered around a given frequency k_0, and propagation either to larger values (for the distribution $\mathcal{T}$) or smaller values (for the distribution $\mathcal{U}$). As an application, we choose

$$\mathcal{T}(k,k_0,Y_0) = \theta(-l) \tag{12}$$

$$\mathcal{U}(k,k_0,Y_0) = \theta(l)\ , \tag{13}$$

where $l \equiv \log\left(k^2/k_0^2\right)$. In section VI, we will examine the dependence on the initial conditions, when they deviate from θ functions[2]. One should also note that the distributions in k-space are no longer probability distributions due to the Fourier transform, and therefore may have magnitudes larger than unity.

---

[2] Note that the initial conditions (12,13) and (4,5) are not Fourier transforms of each other. For instance, the initial condition (5) for $\mathcal{N}$ leads to

$$\mathcal{T}(x_{01},k,Y_0) = \frac{1}{8}\frac{k^2}{k_0^2}\ {}_2F_3\left(1,1;2,2,2;-k^2/4k_0^2\right) + \log\frac{k_0}{k} + \log 2 - \gamma_E\ , \tag{14}$$

where $k_0 = 1/r_0$. This initial condition is not positive definite and diverges in the limit $k \to 0$. We have checked from numerical calculations that these subtleties of the Fourier transforms do not change the overall results.

IV. MINIMAL SIZE DISTRIBUTIONS

Let us first consider the problem of the propagation of the *minimal* size of dipoles. As discussed previously, we shall treat the problem using the Fourier modes of the distribution of sizes.

At $Y = Y_0$, one starts with the θ-function (12) and thus $\mathcal{T} \equiv 1$ for all values $k < k_0$ and zero elsewhere. When the rapidity increases, the splitting of dipoles generates an evolution to smaller and smaller values of r_m, which is reflected upon the Fourier modes by an evolution to larger and larger k. In fact we shall now prove that the solution takes the form of a traveling wave, the wave front defining a critical region around which the size fluctuations giving rise to the maximum of k preferentially occur. We will show that in this case the mathematical arguments developed in [7] prevail.

Let us sketch the arguments of [7] and introduce the Mellin transform with respect to the variable k/k_0. In the long range tail of the distribution $\mathcal{T} \to 0$, the non-linear term in (10) is very small and thus can at first be neglected. The solution of the linear part is

$$\mathcal{T}(k, k_0, Y) \sim \int_{\mathcal{C}} \frac{d\gamma}{2i\pi} \, \frac{1}{\gamma} \, e^{-\gamma l + \omega(\gamma)(Y - Y_0)} \, , \tag{15}$$

where

$$\omega(\gamma) \equiv \frac{\alpha_s N_c}{\pi} \chi(\gamma) = \frac{\alpha_s N_c}{\pi} (2\psi(1) - \psi(\gamma) - \psi(1-\gamma)) \tag{16}$$

is the Mellin transform of the kernel (1) and the prefactor $\frac{1}{\gamma}$ comes from the initial condition (12). We want to look for a wave front and thus search for a specific velocity v_+ characterizing the motion of the wave front. Hence we define a comoving frame defined by the shift $l \to l_{wf} \equiv l - v_+ Y$. A priori, no special velocity v_+ is selected, since for each value of γ one has a velocity $v_+(\gamma) = \frac{\omega(\gamma)}{\gamma}$ to stabilize the value of l_{WF}. However, it can be shown from general grounds [15] that, once the non-linearities are taken properly into account, and provided the initial conditions are steep enough in l, a minimal velocity

$$v_+ = \frac{\omega(\gamma_c)}{\gamma_c} = \min_{\gamma} \frac{\omega(\gamma)}{\gamma} \equiv \omega'(\gamma_c) \tag{17}$$

is selected, in analogy with the group velocity in wave physics [16, 17]. Here $\gamma_c = 0.6275$ is the critical anomalous dimension identical to that found for the BK equation [7, 18]. Note that the initial step function condition (12) for $\mathcal{T}$ is well inside the validity domain $\mathcal{T}(l, Y_0) < e^{-\gamma_c l}, l \gg 0$ required for the traveling wave property to apply.

Hence, from general properties of traveling wave solutions [15], one infers the following for the minimal size distribution: There exists a critical value $k_c(Y)/k_0 \sim r_0/r_c(Y)$ which characterizes the position of the moving wave front of the distributions $\mathcal{T}$ and its Fourier transform $\mathcal{N}$. The value of $k_c(Y)$ is defined as the value of k, at a specified Y, where the distribution $\mathcal{T}$ has a fixed (and small, for consistency) constant value. Since this is also the region where these distributions vary significantly with l, see Fig. 2, $r_c(Y)$ represents the most probable domain value for the minimal dipole size as a function of Y. On general grounds, one may write

$$\frac{r_0}{r_c(Y)} \sim \frac{k_c(Y)}{k_0} \propto \exp\left(v_+ \Delta Y - \frac{3}{2\gamma_c} \log Y \right) , \tag{18}$$

where γ_c and v_+ are given by the solution of the equation (17). The correction $\sim \log Y$ is a universal retardation effect due to the non-linearities [14, 15]. There exists a third $\mathcal{O}(Y^{-1/2})$ sub-asymptotic universal term in the exponential [7] which can be neglected for our purposes.

Together with the front velocity $dk_c(Y)/dY$, it is possible to obtain general knowledge of the front profile in the region next to the tail, including information on the diffusive approach to the scaling curve. It is important to realize that this result comes from the knowledge of the solution of the linearized equation, with the only role of non-linearities being to select the critical regime defined by γ_c. Hence the result can be easily transferred to the inverse Fourier problem, i.e., the original problem of minimal dipole sizes in the evolution. One thus finally finds

$$\mathcal{N}(r_m, Y) \sim \text{const.} \times \sqrt{\frac{2\pi}{N_c \alpha_s \chi''(\gamma_c)}} \log\left(\frac{r_c^2(Y)}{r_m^2} \right) \left(\frac{r_c^2(Y)}{r_m^2} \right)^{-\gamma_c} \exp\left(-\frac{\pi}{2 N_c \alpha_s \chi''(\gamma_c) Y} \log^2\left(\frac{r_c^2(Y)}{r_m^2} \right) \right) \, . \tag{19}$$

All in all, this means that the solution for the minimal size distribution follows the same geometrical scaling solution as the BK S-Matrix. It is governed by the same scaling (and diffusive scaling violation) properties. In this particular case it represents a geometrical feature of minimal-size fluctuations in the dipole wave function, towards the ultraviolet limit (large k or small r).

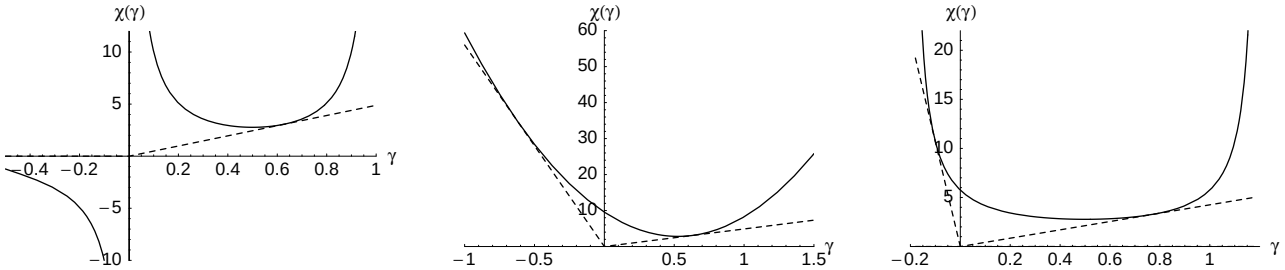

FIG. 3: Graphical solutions of the equation $\chi(\gamma_c) = \gamma_c \chi'(\gamma_c)$, for (a) the LL BFKL kernel, Eq. (16), (b) the diffusive approximation, Eq. (20), and (c) the two-pole approximation, Eq. (22) for $\gamma_0 = 0.2$. For the BFKL kernel there is no solution giving a negative velocity (corresponding to negative γ_c), while for the diffusive and two-pole approximations there are both positive and negative velocity solutions. Note that the magnitude of the negative velocity (i.e. the slope of the tangent) is much larger than for the positive velocity.

V. MAXIMAL SIZE DISTRIBUTIONS

For the maximal size distribution, analyzed in Fourier modes $\mathcal{U}$, the initial condition is specified by (13), which falls among the constraints [7] that eventually generate traveling waves when $l \to -\infty$, if the other mathematical conditions are fulfilled. As discussed above, the speed of the traveling wave is obtained from the equation $v = \gamma_c \chi'(\gamma_c) = \chi(\gamma_c)$, an equation that has only one solution in the case of χ being the leading logarithmic (LL) BFKL kernel. Indeed, χ has poles in $\gamma = 0, 1$, and the unique value of γ_c in the allowed γ-interval is $\gamma_c = 0.6275$, see Fig. 3(a). Hence the analysis of the asymptotic solutions of $\mathcal{U}$ requires a particular treatment. For the moment, let us go back to the original BK equation with known mathematical properties related to its specific non-linear structure.

In Ref. [7], a diffusive approximation of the LL BFKL kernel was considered. This approximation consists in expanding the kernel around $\gamma = \gamma_c$ and keeping terms up to second order,

$$\chi(\gamma) \simeq \chi(\gamma_c) + \chi'(\gamma_c)(\gamma - \gamma_c) + \frac{1}{2}\chi''(\gamma_c)(\gamma - \gamma_c)^2 \qquad \text{(diffusive approx.)}, \tag{20}$$

which brings the BK equation into the form of the Fisher–Kolmogorov–Petrovsky–Piscounov equation [19]. In this kernel there are no poles and the equation for γ_c has two solutions, see Fig. 3(b). This yields forward traveling waves propagating with speed v_+ and backward traveling waves with speed v_-, selected depending on the initial condition [14].

However, for the maximum size distribution we expect that DGLAP or next-to-leading logarithmic (NLL) BFKL effects might be important. Indeed, in some approaches to improving the LL BFKL kernel through resummation of NLL effects [20] or duality with DGLAP evolution [21] the kernel function $\chi(\gamma)$ allows for negative γ_c.

A simple argument for shifting the poles is due to energy conservation: in the relation $\omega = \frac{\alpha_s N_c}{\pi}\chi(\gamma)$, energy conservation translates into the condition that $\omega = 1$ when $\gamma = 0$. In the limit $\gamma \to 0$, the BFKL kernel behaves as $\chi \sim 1/\gamma$, i.e. we may incorporate energy conservation by writing

$$\chi(\gamma) = \frac{1}{\gamma + \frac{\alpha_s N_c}{\pi}} \qquad \text{(small } \gamma\text{)}, \tag{21}$$

which moves the $\gamma = 0$ pole to $\gamma = -\frac{\alpha_s N_c}{\pi}$.

It is well-known that the LL BFKL kernel is well-approximated by a two-pole model, $\chi(\gamma) = 1/\gamma + 1/(1-\gamma)$, which reproduces the poles of the BFKL kernel. This kernel has also been studied in Ref. [22] in the context of saturation and is found to give very similar results as the full kernel.

In view of the above we use as a toy kernel

$$\chi(\gamma) = \frac{1}{\gamma + \gamma_0} + \frac{1}{1 - \gamma + \gamma_0} + 4\left(\log 2 - \frac{1}{1 + 2\gamma_0}\right), \tag{22}$$

which reproduces the main features of the BFKL kernel with the poles at $\gamma = 1$ and $\gamma = 0$ shifted by an amount γ_0 and $-\gamma_0$ respectively. We consider γ_0 as a free parameter of our model. This kernel can be viewed as an approximation of some next-to-leading effects, and is also simple enough to use in our reasoning. The constant term is chosen to reproduce the value of the full BFKL kernel at $\gamma = 1/2$.

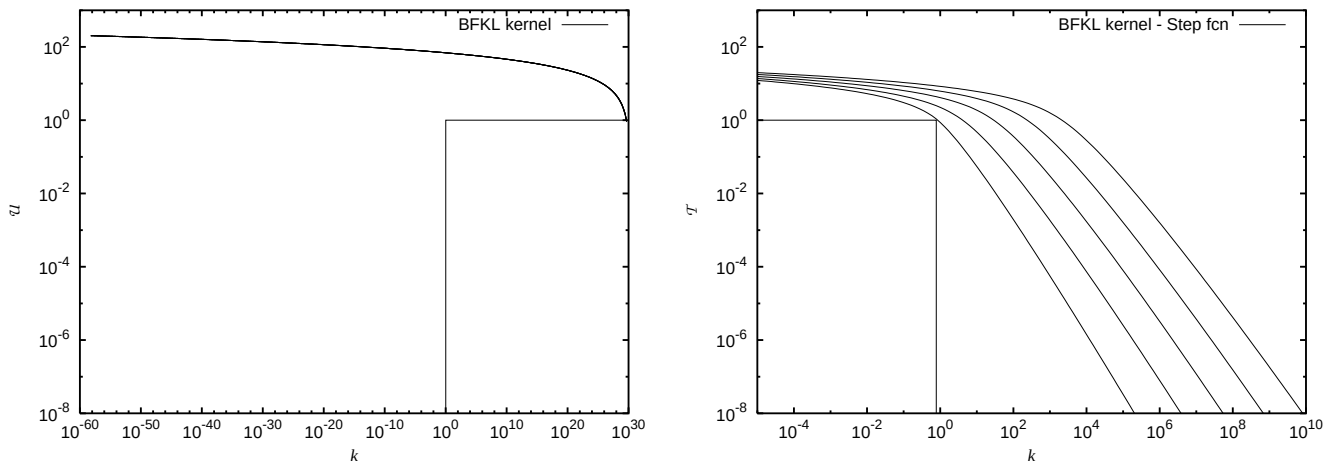

FIG. 4: Evolution of extremal Fourier modes for the LL BFKL kernel. Left: towards the infrared; Right: towards the ultraviolet. The rapidity steps are $\delta Y = 1$. In the left plot, all lines with $Y \neq 0$ scale on the same curve.

For example, choosing the value $\gamma_0 = 0.2$, one obtains two real solutions to the equation defining γ_c, $\gamma_c^+ = 0.766$ and $\gamma_c^- = -0.103$, corresponding to a positive and a negative velocity, as illustrated in Fig. 3(c). All these examples will now be discussed by comparison with numerical simulations.

VI. NUMERICAL SIMULATIONS

The BK equation has been solved numerically by many groups, by direct solution of the integro-differential equation. Recently, in Ref. [22], it was solved using a discretization of the integrand through Chebyshev approximation and a Runge–Kutta method for the ensuing system of ordinary differential equation (see [22] for more details on the method). The solutions were studied in detail and compared to analytical results obtained using the traveling wave front method. In this paper we use the same numerical method to study the solutions for the distributions $\mathcal{T}$ and $\mathcal{U}$ in k-space.

First let us consider the simulation of equation (10) made using the original BFKL kernel (11), corresponding to the case of Fig. 3(a).

It is remarkable that traveling wave solutions are generated in the forward direction, while the backward direction is characterized by a scaling curve. In LL BFKL, hence, there are only forward traveling waves. The backward solution does not propagate at high Y, but instead there is a fixed scaling solution (in a sense the speed is infinite and the wave front is situated at $l = -\infty$). This situation is illustrated in Fig. 4.

In order to analyze in more detail this backward scaling, we considered the same problem with smaller steps in rapidity, see Fig. 5. We see the evidence for a diffusive evolution towards the scaling curve. Note also the instability of the far infrared region, which is immediately reached by the evolution. This is a feature related to the singularity of the canonical BFKL case at $\gamma = 0$, and, as we shall see now, is resolved by next leading corrections. This sensibility to next leading QCD corrections is an interesting feature of backward propagation towards the infrared.

In Fig. 6, we show the similar plot for the non-linear evolution using the two-pole kernel (22) with different values of the parameter γ_0 which, in our toy model, schematically characterize the amount of next-leading corrections. Interestingly enough, the toy model results for $\gamma_0 = 0$ reproduce the same features as for the BFKL kernel, with a scaling curve in the backward propagation. For non-zero $\gamma_0 = 0.2, 0.4$, left-moving traveling waves appear, in agreement with the analytical predictions. In all cases the speed is faster than for the forward propagation (i.e. faster than the BK traveling waves). Hence the infrared instability is made finite but the maximal evolution towards the infrared is rapid: large dipole sizes are easily produced in the energy evolution. The comparison between the forward and backward evolutions is exemplified in Fig. 7.

To round up the numerical results we give an example of the (in)dependence of the traveling wave regime from

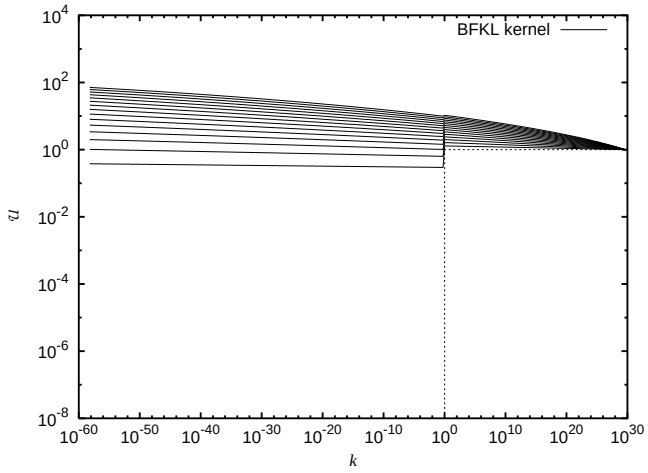

FIG. 5: BFKL evolution towards the infrared. The rapidity steps are $\delta Y = 0.1$

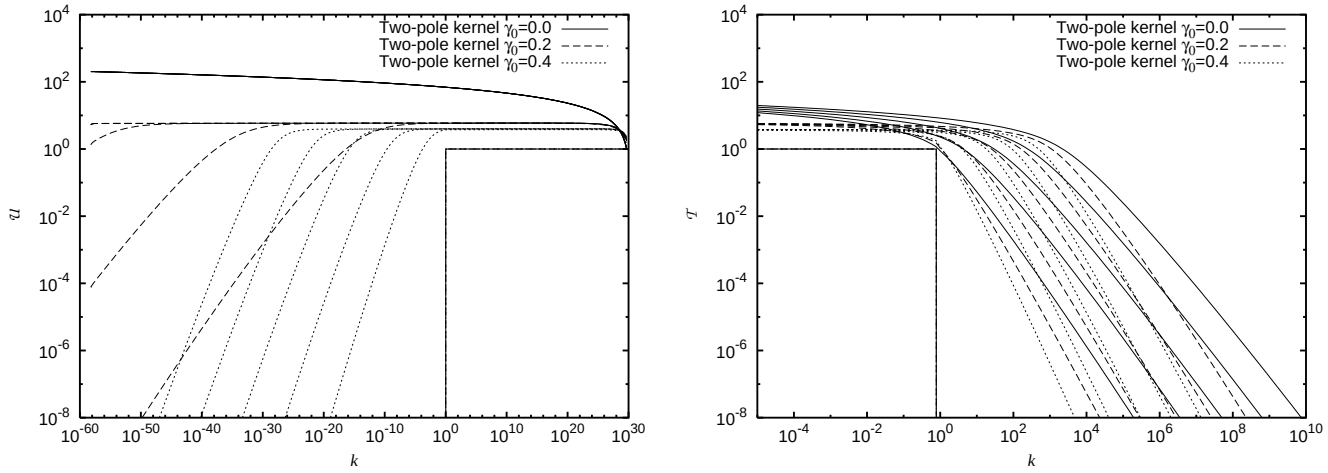

FIG. 6: Evolution of extremal Fourier modes for the two-pole model. Left: towards the infrared; Right: towards the ultraviolet. The curves are drawn for values $\gamma_0 = 0, 0.2, 0.4$ and the rapidity steps are $\delta Y = 1$.

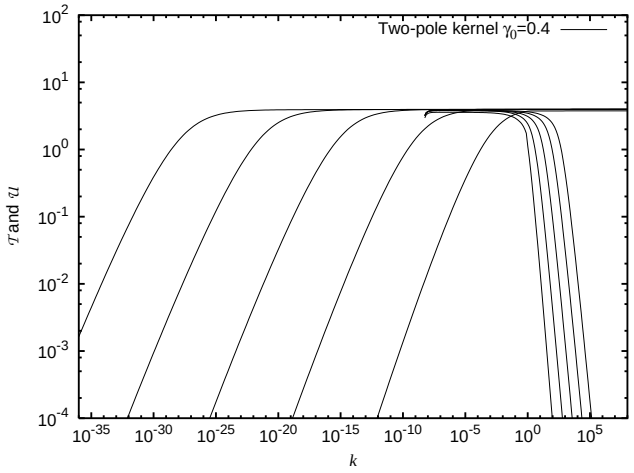

FIG. 7: Comparison of forward and backward Evolution for $\gamma_0 = 0.4$. The rapidity steps are $\delta Y = 1$

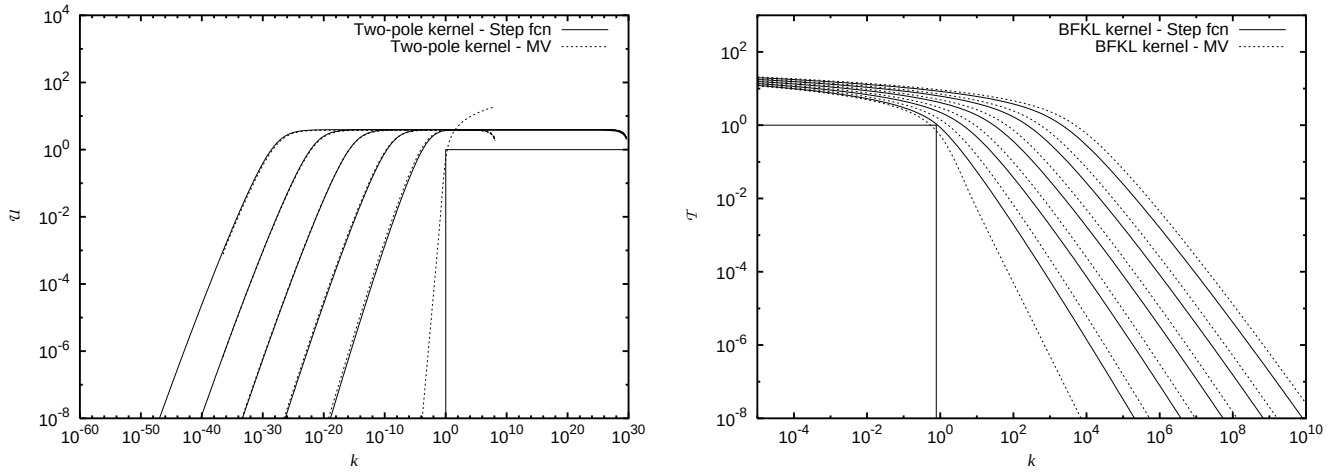

FIG. 8: Evolution of extremal Fourier modes for different initial conditions. Left: two-pole model towards the infrared; Right: BFKL kernel towards the ultraviolet. Continuous lines: initial step functions. Dotted lines: McLerran–Venugopalan form (see text).The curves are drawn for the BFKL kernel and the rapidity steps are $\delta Y = 1$.

initial conditions by comparing initial step functions with a form inspired by[3] the McLerran–Venugopalan model [23]. As typical examples (see Fig. 8) we considered the backward waves obtained for the toy model and the forward waves for the original BFKL kernel.

Finally, we confirm that the speed of the front propagation is correctly given by the analytical formula for asymptotically large rapidities, i.e., we compare the rapidity dependence of the saturation scale of the forward and backward traveling waves obtained from the numerical solution to the analytical formula for asymptotically large rapidities.

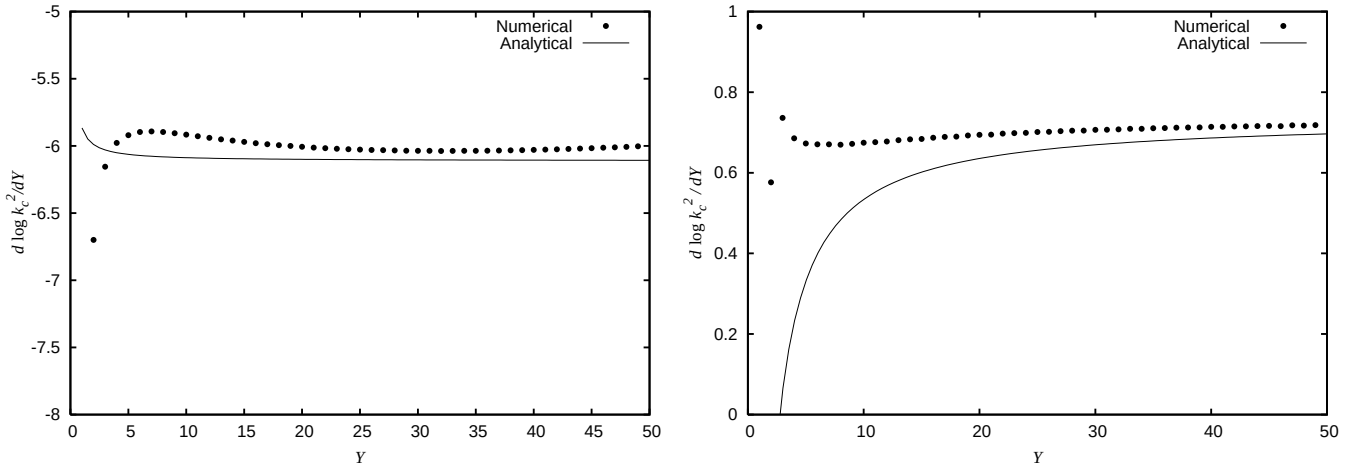

FIG. 9: Comparison of the analytical form for the derivative in (24) with the results from the numerical simulation, for backward evolution (left) and forward evolution (right). The equation analyzed here is given by the the two-pole toy kernel (22) with $\gamma_0 = 0.4$.

The saturation scale $k_c(Y)$ is defined as the momentum, at a certain rapidity, where the amplitude reaches a particular value κ, i.e., $\mathcal{N}(k_c(Y), Y) = \kappa$. The overall normalization therefore depends on the chosen value of κ and it is most convenient to study the logarithmic derivative of $k_c(Y)$, where the normalization cancels. Because the shape

[3] In practice we used the numerical Fourier transform of the McLerran–Venugopalan distribution given in r-space by

$$1 - \exp\left(-r^2 Q_s^2(Y)/4 \log[e + 1/(r^2\Lambda^2)]\right) \ . \tag{23}$$

of the front is not completely fixed as it propagates in rapidity, the functional form of $\partial \log k_c(Y)/\partial Y$ will also depend on κ, but this dependence is a subleading effect in Y and vanishes as Y becomes large[4]. Here we choose $\kappa = 0.01$.

The analytical result given by (18) is

$$\frac{\partial \log k_c(Y)}{\partial Y} = v_+ - \frac{3}{2\gamma_c Y}, \tag{24}$$

where subleading $\mathcal{O}(Y^{-3/2})$ terms have been omitted. Fig. 9 shows the results of the comparison between the simulations and expression (24) for the two-pole toy kernel (22) with $\gamma_0 = 0.4$ (the constants are given by Eq. (17): $v_+ = 0.7372$, $v_- = -6.112$, $\gamma_+^c = 0.9157$, and $\gamma_-^c = -0.2202$). The results indicate that the two results tend to the same asymptotic values $v_\pm$ of the derivative, while there are still appreciable subasymptotic effects [22].

VII. CONCLUSIONS AND OUTLOOK

Let us summarize the results obtained in our study of size fluctuations during QCD dipole cascading.

The extremal size probability distributions are shown to obey non-linear evolution equations as a function of rapidity. These equations are formally of the BK form and thus their asymptotic solutions can be obtained following the general mathematical recipes for non-linear equations of the same universality class.

The *minimal* size distribution has initial conditions which imply traveling wave solutions of the same type as for the BK equation for saturation. In particular the rate of evolution towards the ultraviolet is the same as the saturation scale evolution.

The *maximal* size distribution shows new and distinctive features which have not been discussed in this way previously, due to specific initial conditions. In the case of the BFKL kernel, i.e. in the leading log approximation of perturbative QCD, one obtains a fixed scaling distribution (after a short diffusive interlude) which extends towards the far infrared region. This phenomenon is due to the singularity of the BFKL kernel at $\gamma = 0$. As soon as this singularity is shifted or smoothed out, new traveling-wave solutions appear, with a (fast) speed of backward propagation towards large sizes, i.e. the infrared. In particular, next-to-leading corrections to the BFKL kernel gives rise to such a phenomenon and determine the value of the critical speed.

These analytical predictions have been verified by numerical solutions of the evolution equations which have been treated here by looking to the Fourier modes of the dipole sizes.

Let us note that these results have been obtained assuming a fixed value of the coupling constant. They have a natural extension to running coupling, using the method of Ref.[7] for solutions of the BK equation with running coupling. We expect qualitatively similar results but the quantitative analysis deserves to be performed.

One should emphasize that these are features of the QCD dipole cascade derived from the *linear* BFKL regime. Its non-linear features are related to the structure of maximal fluctuations around the mean, even if formally they take the form of a saturation equation. It is quite interesting to imagine what could be the effect of saturation on these fluctuations. It will probably damp considerably the evolution towards the infrared and thus give rise to a stabilization of the solution by moderating the fluctuations to large dipole sizes.

The discussion of fluctuations towards the ultraviolet seems to be more subtle. It is nowadays emphasized [13] that these fluctuations could sizably modify the saturation solutions, violate geometric scaling or even back-react onto the linear regime. What we obtain from our analysis of minimal size fluctuations is that they propagate with the same speed as the saturation scale, i.e. the dominant scale in a saturation regime without large fluctuations. Thus one expects to find fluctuations a finite comoving distance ahead of the mean field solution. It will be quite interesting to analyze the structure of such a "fluctuation shell" and its effect on the whole system. Perhaps more properties borrowed (and modified) from statistical physics could help clarifying this problem.

---

[4] See [22] for examples and a thorough discussion.

Acknowledgments

We thank A. Bialas, K. Golec-Biernat C. Marquet and G. Soyez for fruitful discussions and careful reading of the manuscript. R.P. wishes to thank S. Majumdar for an inspiring seminar (and work) on statistical physics.

---

[1] L. N. Lipatov, Sov. J. Nucl. Phys. **23** (1976) 338;
E. A. Kuraev, L. N. Lipatov, and V. S. Fadin, Sov. Phys. JETP **45** (1977) 199;
I. I. Balitsky and L. N. Lipatov, Sov. J. Nucl. Phys. **28** (1978) 822.
[2] A. H. Mueller, Nucl. Phys. **B415** (1994) 373;
A. H. Mueller and B. Patel, Nucl. Phys. **B425** (1994) 471;
A. H. Mueller, Nucl. Phys. **B437** (1995) 107.
[3] N. N. Nikolaev and B. G. Zakharov, Z. Phys. **C49** (1991) 607.
[4] For a review on saturation and references, see e.g. A. H. Mueller, hep-ph/0111244.
[5] I. I. Balitsky, Nucl. Phys. B **463** (1996) 99 [arXiv:hep-ph/9509348];
I. Balitsky, arXiv:hep-ph/0101042.
[6] Y. V. Kovchegov, Phys. Rev. **D60** (1999) 034008 [arXiv:hep-ph/9901281];
Y. V. Kovchegov, Phys. Rev. **D61** (2000) 074018 [arXiv:hep-ph/9905214].
[7] S. Munier and R. Peschanski, Phys. Rev. Lett. **91** (2003) 232001 [arXiv:hep-ph/0309177];
S. Munier and R. Peschanski, Phys. Rev. D **69** (2004) 034008 [arXiv:hep-ph/0310357];
S. Munier and R. Peschanski, Phys. Rev. D **70** (2004) 077503 [arXiv:hep-ph/0401215].
[8] A. M. Staśto, K. Golec-Biernat, and J. Kwieciński, Phys. Rev. Lett. **86** (2001) 596 [arXiv:hep-ph/0007192].
[9] G. P. Salam, Nucl. Phys. B **461** (1996) 512 [arXiv:hep-ph/9509353];
G. P. Salam, Comput. Phys. Commun. **105** (1997) 62 [arXiv:hep-ph/9601220];
A. H. Mueller and G. P. Salam, Nucl. Phys. B **475** (1996) 293 [arXiv:hep-ph/9605302].
[10] E. Levin and K. Tuchin, Nucl. Phys. B **573** (2000) 833 [arXiv:hep-ph/9908317];
E. Levin and K. Tuchin, Nucl. Phys. A **691** (2001) 779 [arXiv:hep-ph/0012167].
[11] A. H. Mueller and E. Iancu, Nucl. Phys. A **730** (2004) 494 [arXiv:hep-ph/0309276].
[12] J. Jalilian-Marian, A. Kovner, A. Leonidov and H. Weigert, Nucl. Phys. B **504** (1997) 415 [arXiv:hep-ph/9701284];
J. Jalilian-Marian, A. Kovner, A. Leonidov and H. Weigert, Phys. Rev. D **59** (1999) 014014 [arXiv:hep-ph/9706377];
H. Weigert, Nucl. Phys. A **703** (2002) 823 [arXiv:hep-ph/0004044];
E. Iancu, A. Leonidov and L. D. McLerran, Nucl. Phys. A **692** (2001) 583 [arXiv:hep-ph/0011241];
E. Iancu, A. Leonidov and L. D. McLerran, Phys. Lett. B **510** (2001) 133 [arXiv:hep-ph/0102009];
E. Ferreiro, E. Iancu, A. Leonidov and L. McLerran, Nucl. Phys. A **703** (2002) 489 [arXiv:hep-ph/0109115].
[13] A. H. Mueller and A. I. Shoshi, Nucl. Phys. B **692** (2004) 175 [arXiv:hep-ph/0402193];
E. Iancu, A. H. Mueller and S. Munier, arXiv:hep-ph/0410018;
E. Levin and M. Lublinsky, Phys. Lett. B **607** (2005) 131 [arXiv:hep-ph/0411121];
E. Iancu and D. N. Triantafyllopoulos, arXiv:hep-ph/0411405;
A. H. Mueller, A. I. Shoshi and S. M. H. Wong, arXiv:hep-ph/0501088;
E. Iancu and D. N. Triantafyllopoulos, arXiv:hep-ph/0501193.
[14] P. L. Krapivsky and S. N. Majumdar, Phys. Rev. Lett. **85** (2000) 5492 [arXiv:cond-mat/0006117];
S. N. Majumdar and P. L. Krapivsky, Phys. Rev. E **62** (2000) 7735 [arXiv:cond-mat/0006236];
D. S. Dean and S. N. Majumdar, Phys. Rev. E **64** (2001) 046121 [arXiv:cond-mat/0104028];
S.N. Majumdar and P.L. Krapivsky, Phys. Rev. E **63** (2001) 045101;
for a recent brief review of these results see S.N. Majumdar and P.L. Krapivsky, Physica A **318** (2003) 161 [arXiv:cond-mat/0205581].
[15] U. Ebert, W. van Saarloos, Physica **D 146** (2000) 1 [arXiv:cond-mat/0003181];
for a review, see W. van Saarloos, Phys. Rep. **386** (2003) 29.
[16] L.V. Gribov, E.M. Levin and M.G. Ryskin, Phys. Rep. **100** (1983) 1.
[17] E. Levin, J. Bartels, Nucl. Phys. **B387** (1992) 617.
[18] E. Iancu, K. Itakura and L. McLerran, Nucl. Phys. **A708** (2002) 327 [arXiv:hep-ph/0203137].
[19] R. A. Fisher, Annals Eugen. **7** (1937) 355;
A. Kolmogorov, I. Petrovsky, and N. Piscounov, Moscou Univ. Bull. Math. **A1** (1937) 1; reprinted in P. Pelcé, *Dynamics of Curved Fronts* (Academic Press, San Diego, 1988).
[20] M. Ciafaloni, D. Colferai and G. P. Salam, Phys. Rev. D **60** (1999) 114036 [arXiv:hep-ph/9905566];
M. Ciafaloni, D. Colferai and G. P. Salam, JHEP **9910** (1999) 017 [arXiv:hep-ph/9907409];
M. Ciafaloni, D. Colferai, G. P. Salam and A. M. Staśto, Phys. Rev. D **68** (2003) 114003 [arXiv:hep-ph/0307188].
[21] G. Altarelli, R. D. Ball, S. Forte, Nucl. Phys. **B621** (2002) 359 [arXiv:hep-ph/0109178], and references from the same authors therein.
[22] R. Enberg, K. Golec-Biernat, S. Munier, in preparation.
[23] L. D. McLerran and R. Venugopalan, Phys. Rev. D **50** (1994) 2225 [arXiv:hep-ph/9402335].